Photomechanical Control of the Electronic Properties of Linear π-Conjugated Systems

Bruno Jousselme,[a] Philippe Blanchard,*[a] Nuria Gallego-Planas,[b] Eric Levillain,[a] Jacques Delaunay,[b] Magali Allain,[b] Pascal Richomme,[c] and Jean Roncali*[a]

Abstract: Photodynamic molecular architectures have been synthesized by covalent fixation of a photoisomerizable dimethylazobenzene group at two fixed points of conformationally flexible π-conjugated quater- and sexithiophene chains. Theoretical geometry optimization shows, in excellent agreement with crystallographic structures, that the mode of fixation of the azo group plays a determining role in the geometry of the final molecular architecture and on its ability to perform the expected photoinduced molecular motion. Thus, covalent fixation of *meta*-dimethylazobenzene on a quaterthiophene chain results in a conformationally locked system in which photoisomerization of the azo group is hindered. However, the experimental results of optical, ^{1}H NMR spectroscopic, and electrochemical investigations show that when an azobenzene group is connected at the *para* positions of the phenyl rings, *trans*-to-*cis* photoisomerization of the azo group induces a conformational transition and dimensional changes in the underlying π-conjugated oligothiophene chain. These experimental results unequivocally show that the photochemically induced geometrical changes produce in turn an increase in the HOMO level and a narrowing of the HOMO–LUMO gap. This therefore provides the first evidence of photomechanical control of the electronic properties of linear π-conjugated systems.

Keywords: azo compounds · molecular actuation · nanostructures · oligothiophenes · photochemistry

Introduction

The synthetic chemistry of nanoscale molecular devices is acquiring an increasing importance in the rapidly expanding field of nanosciences. In addition to the continuing development of molecular wires,[1] rectifiers,[2] switches,[3]or logic gates,[4] the recent emergence of dynamic molecular devices[5] opens a new field of research in the chemistry of nano-objects. Thus, in the past few years, molecular architectures such as gears,[6] shuttles,[7] ratchets,[8] motors,[9] and muscles[10] capable of converting thermal, chemical, or photochemical energy into molecular motion and hence mechanical energy have been described. Such molecular machines and motors are thought to pave the way toward the development of the futuristic field of nanorobotics.

Initial prototypes of molecular machines capable of producing a repeatable and directionally controlled motion were essentially powered by means of changes in the oxidation state of a mobile part of the molecular architecture. Thus, Stoddart and co-workers have developed molecular shuttles in which modifications of the oxidation state of a redox-active system embedded in a rotaxane induces its translocation along a linear axis.[7a] Sauvage and co-workers have synthesized molecular machines and muscles powered by chemically or electrochemically induced changes of the redox state and hence coordination sphere of a metal complexed in rotaxanes containing tetra- and pentacoordination sites.[7b]

Among the various possible power sources for molecular dynamic devices, light presents a number of specific advantages such as rapid, easy, and direct access to the target active site of the system and the absence of foreign chemicals. Some examples of photochemically powered molecular machines have already been described and, in particular, Ferringa and co-workers have synthesized molecular machines that undergo circular motion,[9] while Hugel et al. have investigated a polymeric system that undergoes a single-molecule optomechanical cycle.[11]

Thiophene-based monodisperse π-conjugated oligomers have been widely investigated as active materials in field-

[a] Dr. P. Blanchard, Dr. J. Roncali, Dr. B. Jousselme, Dr. E. Levillain
Groupe Systèmes Conjugués Linéaires
UMR CNRS 6501, Université d'Angers
2 boulevard Lavoisier, 49045 Angers (France)
Fax: (+33) 2-41-73-54-05
E-mail: philippe.blanchard@univ-angers.fr
jean.roncali@univ-angers.fr

[b] N. Gallego-Planas, Dr. J. Delaunay, M. Allain
Ingénierie Moléculaire et Matériaux Organiques
UMR CNRS 6501, Université d'Angers
2 boulevard Lavoisier, 49045 Angers (France)

[c] Prof. P. Richomme
Service Commun d'Analyses Spectroscopiques, Université d'Angers
2 boulevard Lavoisier, 49045 Angers (France)

 DOI: 10.1002/chem.200305010

effect transistors or light-emitting diodes.[12, 13] Although these oligomers have also been considered as molecular wires for molecular electronic devices,[1, 14] their possible use in dynamic nanosystems has scarcely been considered so far. Bulk electrochemical actuators based on the volume changes associated with the doping/dopant-removal process of conjugated polymers have been known for some time,[15] but the molecular parent systems are still to be developed. Marsella et al. recently reported a first step in this direction by investigating a model of a molecular actuator based on poly[cyclooctatetrathiophene].[16]

Recently, we have shown that response to stimulation of a sensitive group covalently attached at two fixed points of an oligothiophene (nT) chain allows a novel concept relevant for both molecular actuation and molecular electronics to be developed. In fact, such as stimuli-responsive system can be used to indirectly generate reversible conformational changes in the π-conjugated system.[17]

The interest of this approach is twofold. Because the π-conjugated system is the target of the generated molecular motion, it represents an interesting optical and redox probe allowing the real-time monitoring of the produced movement by simple electrochemical and optical techniques. Furthermore, because of the high sensitivity of the electronic properties of linear π-conjugated systems on deviation from planarity,[18] this concept makes it possible to achieve an indirect mechanical control of the electronic properties of the conjugated system by stimulation of the attached driving group.

The validity of this approach was first demonstrated for crown-annealed nTs built by fixing a polyether loop to two fixed points of an nT chain. Theoretical and experimental analyses showed that in that case cation-binding induces a conformational transition in the π-conjugated system, which in turn produces reversible changes in its electronic properties.[17]

In a recent short communication we reported an extension of the same concept in which a photoactuating governor was used to achieve a photomechanical conformational switch between two electronically different states of a π-conjugated nT chain.[19]

As the photoactive driving group we used the azobenzene chromophore, which can be reversibly switched at two different wavelengths between an extended *trans* and a shorter *cis* configuration.[20] This property has been widely used to achieve stimulus-response-based control over the electronic properties of conjugated polymers[21] and dendrimers.[22]

As a next step, we report here further investigations on the design, synthesis, structure, and photodynamic properties of this new class of dynamic π-conjugated systems. The effects of the mode of attachment of the azobenzene group (*meta* or *para*) have been investigated by theoretical modeling and X-ray crystallographic structural analysis of compounds *m*-**4T** and *p*-**4T**. A longer system based on sexithiophene (*p*-**6T**) was also synthesized in order to confirm the possible generalization of this new approach to longer molecular wires.

The photodynamic behavior of these various compounds has been investigated by a joint theoretical and experimental study. Results of optical, NMR spectroscopic, and electrochemical investigations provide consistent results that unequivocally demonstrate photomechanical control of the electronic properties of the π-conjugated system through photoactuation.

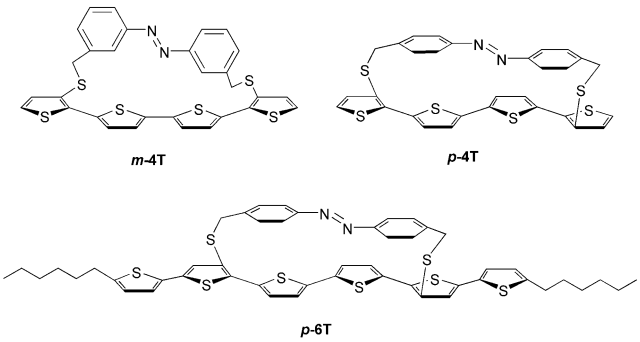

Results and Discussion

Synthesis: The target azobenzene-derivatized quater- and sexithiophenes *m*-**4T**, *p*-**4T**, and *p*-**6T** were synthesized according to the procedures depicted in Scheme 1. Our strategy involves the preparation of an oligothiophene with two protected thiolate groups at defined positions of the conjugated chain.[17, 23] The target compounds are then obtained in one pot by deprotection of the thiolate functionality

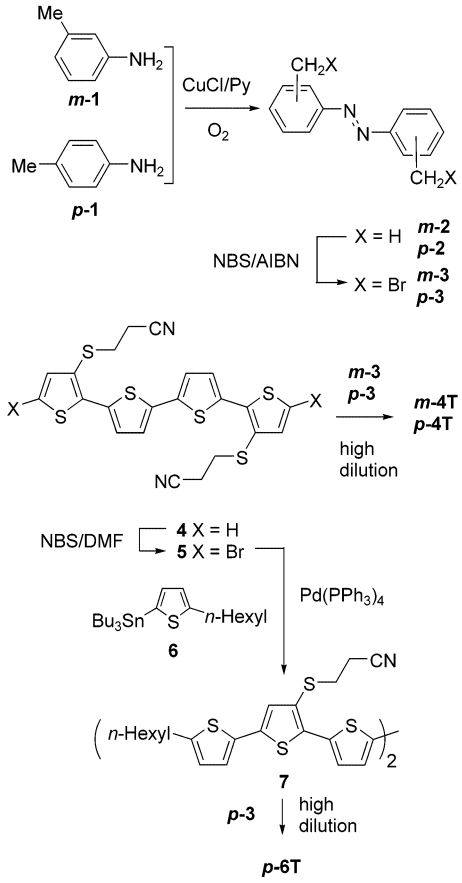

Scheme 1.

with cesium hydroxide[24] and ring closure by treatment with a bis(bromomethyl)-derivatized azobenzene.

Meta- and *para*-bis(bromomethyl)-azobenzenes (*m*-**2**) and (*p*-**2**) were prepared in 44 and 32% yield, respectively, by oxidative coupling of *meta*-toluidine (*m*-**1**) and *para*-toluidine (*p*-**1**) in the presence of Cu_2Cl_2 and oxygen.[25] Radical bromination of *m*-**2** and *p*-**2** by using *N*-bromosuccinimide (NBS) in DMF in the presence of (azobisisobutyronitrile) AIBN or benzoylperoxide led to bis(bromomethyl)azobenzenes *m*-**3** and *p*-**3** in 30% yield. Bis(cyanoethylsulfanyl)quaterthiophene **4**, prepared according to the method already described,[23] was treated with bis(bromomethyl)azobenzenes *m*-**3** and *p*-**3** under high-dilution conditions to give the targets quaterthiophenes *m*-**4T** and *p*-**4T** in 63% and 18% yield, respectively.

Bromination of **4** with NBS in DMF gave dibromoquaterthiophene **5** in 62% yield. Commercially available 2-hexylthiophene was treated with butyllithium and tributyltin chloride to afford 2-(tributylstannyl)-5-hexylthiophene (**6**) (yield 98%). A Stille coupling reaction between compounds **5** and **6** in the presence of a palladium catalyst led to bis(cyanoethylsulfanyl)sexithiophene **7** in 26% yield. This compound was subsequently treated with bis(bromomethyl)azobenzene *p*-**3** to give the target compound *p*-**6T** in 17% yield. All compounds were fully characterized by ^{1}H and ^{13}C NMR spectroscopy, mass spectrometry, and elemental analysis, which gave satisfactory results.

Theoretical study: Theoretical calculations of the electronic structure and optimal geometry of compounds *m*-**4T** and *p*-**4T** were performed by using density functional methods. All geometries were optimized with hybrid functionals (Becke's three-parameter gradient-corrected functional) and a polarized 6-31G* basis for all atoms with the Gaussian 98 program.[26]

The geometries of the model compounds of the various constitutive building blocks of the systems, namely *meta*- and *para*-dimethylazobenzenes *m*-**2** and *p*-**2** and 3,3‴-dimethylsulfanylquaterthiophene (Me_2**4T**) were first optimized independently.

As suggested by Figure 1, *trans*-to-*cis* isomerization of the azo group should result in a decrease of the distance between the carbon atoms of the two methyl groups from 9.2 to 6.1 Å for *m*-**2** and from 12.1 to 8.6 Å for *p*-**2**.

On the other hand, examination of the optimized geometries corresponding to the energy minima found for the different possible conformers of MeS_2**4T** shows that the distance between the two sulfur atoms serving as possible anchoring points for the azobenzene group decreases from the *syn-anti-syn* conformation (***SAS***) to the ***ASA*** one in the following order ***SAS*** (12.1 Å) > ***SSS*** (11.2 Å) > ***AAA*** (10.8 Å) > ***SSA*** (10.7 Å) > ***AAS*** (10.3 Å) > ***ASA*** (7.5 Å). Contrary to what could be intuitively expected, the ***AAA*** conformation usually observed for unsubstituted *n*Ts[27] does not lead to the greatest distance between the sulfide groups.

Comparison of the various sulfur–sulfur distances to those found between the two methyl groups of *trans*- and *cis*-dimethylazobenzenes *m*-**3** and *p*-**3** clearly shows that the S···S distances in the ***SAS*** and ***ASA*** conformations of MeS_2**4T** (Figure 1) represent the best fit for *trans*- and *cis*-*p*-**3**, respectively. On the other hand, the ***ASA*** conformation appears to be the only possibility for *trans*-*m*-**3**. Since this conformation corresponds to the smallest S···S distance, it can already be anticipated that isomerization of the azo group will be severely hindered in the assembled *m*-**4T** system.

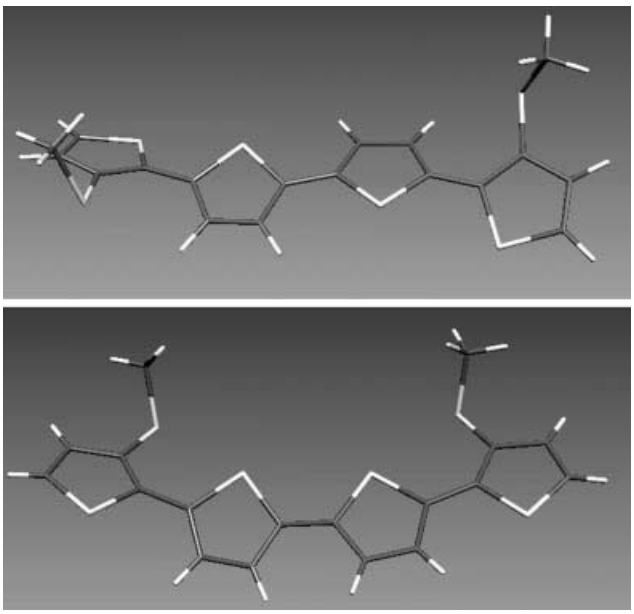

Figure 1. Geometry optimization for MeS_2**4T.** Top: ***SAS*** conformation, bottom: ***ASA*** conformation.

Figure 2 shows the theoretically optimized structures of the complete molecules of *m*-**4T** and *p*-**4T**. The structure of *m*-**4T** (top) shows that the *trans* azo group lies in a plane orthogonal to that of the 4T chain. The latter adopts a quasiplanar geometry with the expected ***ASA*** conformation. Optimization predicts a quite different geometry for *p*-**4T**. The 4T chain deviates slightly from planarity with the sulfur atoms of the terminal thiophene rings pointing upward and downward in order to maximize the distance between the sulfide S atoms. Nevertheless, the azo group appears slightly bent; this suggests that a constraint persists. In sharp contrast to *m*-**4T**, the two conjugated systems now lie in parallel planes.

When the azobenzene group is in its *trans* configuration, the 4T chain adopts a ***SAS*** conformation and undergoes a transition to the ***ASA*** geometry upon *trans*-to-*cis* photoisomerization of the driving azo group. These results show that the fixation of the *trans* azo group results in an increase of the S···S distance from 10.8 Å (for the usual ***AAA*** conformation of *n*Ts), to 12.1 Å for the ***SAS*** one, while the ***SAS***-to-***ASA*** transition produces a decrease of this distance to 7.5 Å. Computations also show that the *trans*-azobenzene-***SAS*** isomer of *p*-**4T** is more stable than the *cis*-azobenzene-***ASA*** one by 52.6 kJ mol^{-1}.

The electronic structure of the optimized geometry of *p*-**4T** was also investigated, and showed that the ***SAS***-to-***ASA*** conformational transition increases the HOMO level from −5.10 to −5.02 eV and decreases the HOMO–LUMO gap from 3.24 to 3.03 eV. However, further analysis of the atomic

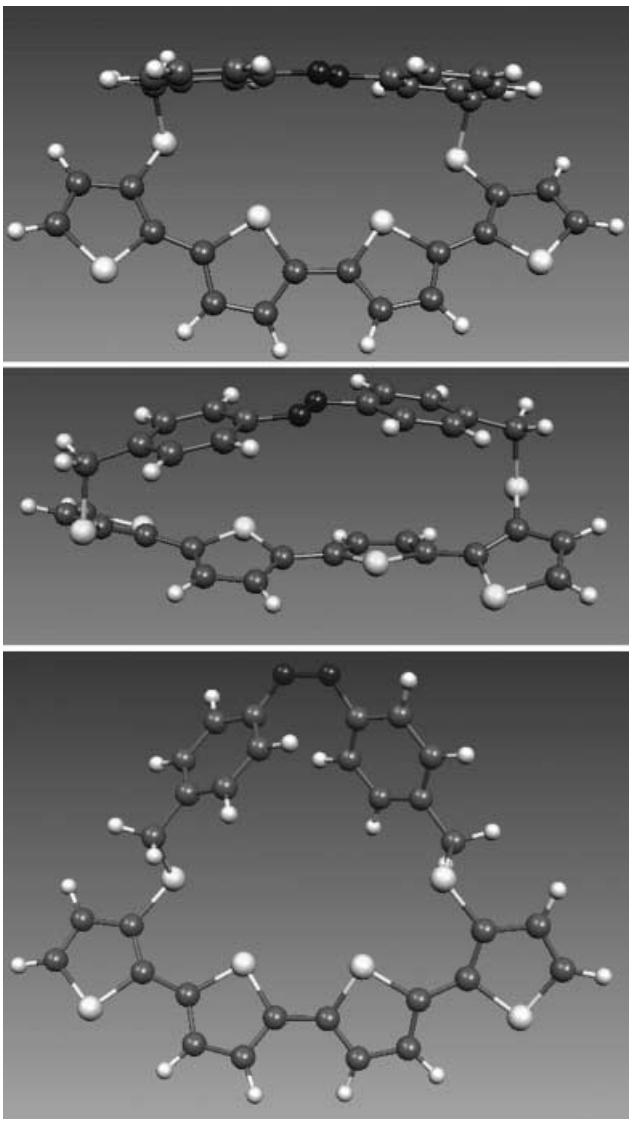

Figure 2. Optimized geometries for *m*-**4T** (top), *trans*-*p*-**4T** (middle), and *cis*-*p*-**4T** (bottom).

contributions to the LUMO shows that this orbital is essentially localized on the azo group (Figure 3), and it is therefore necessary to consider the HOMO – (LUMO + 1) gap in order to evaluate the changes induced by the conformational switch in the electronic properties of the 4T chain.

Crystallographic analysis: Figure 4 shows the crystallographic structures of single crystals of *p*-**4T** and *m*-**4T**. In both cases the X-ray structure agrees well with the conclusions of molecular modeling. For *m*-**4T**, the 4T chain adopts the expected ***ASA*** conformation, while the 4T and azobenzene systems lie in almost perpendicular planes. The azobenzene system remains perfectly planar, while the two end thiophene rings of the 4T chain present a small dihedral angle relative to the central bithiophene core. The S1 ··· S6 distance of 8.5 Å is in satisfying agreement with the theoretically predicted value of 7.5 Å. It is worth noting that the observed ***ASA*** conformation exactly corresponds to that expected for *p*-**4T** after *trans*-to-*cis* isomerization of the azo group. For *p*-**4T**, the X-ray structure confirms the small deviation from planarity predicted for the 4T chain and the slightly bent structure of the azo group. The 4T chain adopts the expected ***SAS*** conformation, and the 12.3 Å distance found between the two sulfur atoms bearing the azobenzene group is in excellent agreement with the theoretically predicted value of 12.1 Å. The two conjugated systems lie in two quasiparallel planes with an average spacing of 3.6 Å.[19] Based on these strongly different relative orientations of the azo and 4T systems in *p*-**4T** and *m*-**4T**, markedly different interactions between the two conjugated systems can be anticipated.

Despite several attempts, single crystals of *p*-**6T** of sufficient quality for X-ray structural analysis could not be obtained. However, based on theoretical results and on the X-ray structure of *p*-**4T**, it seems reasonable to assume that the position of the azo group relative to the *n*T chain is similar to that found in *p*-**4T**.

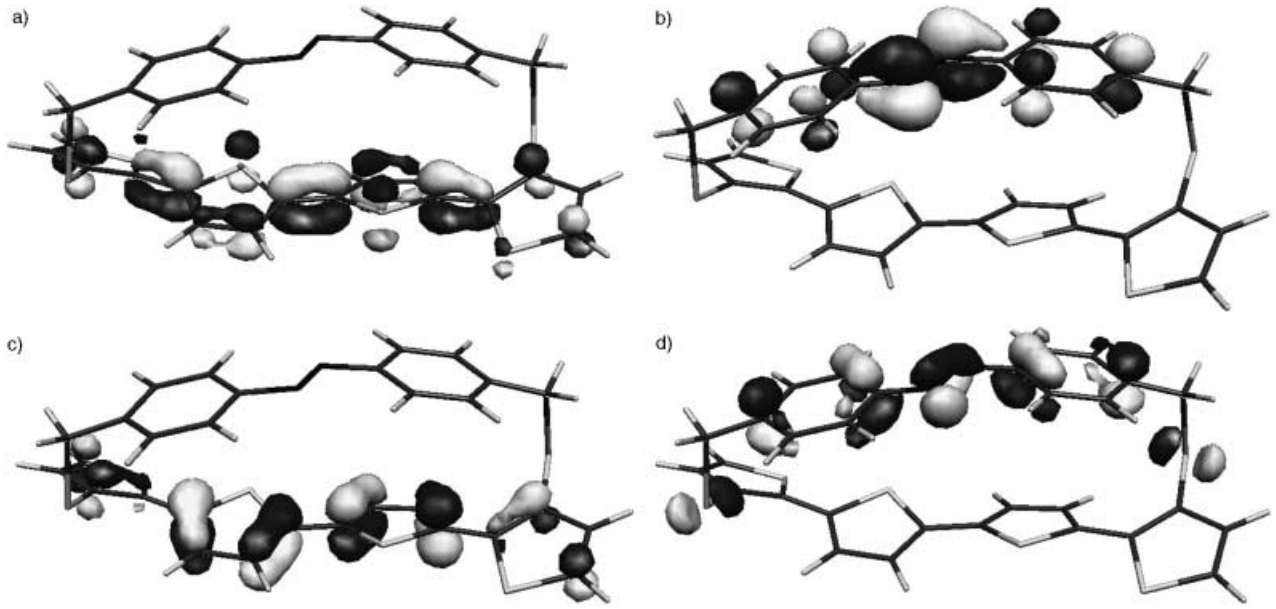

Figure 3. Orbitals of *p*-**4T**. a) LUMO + 1, b) LUMO, c) HOMO, d) HOMO – 1.

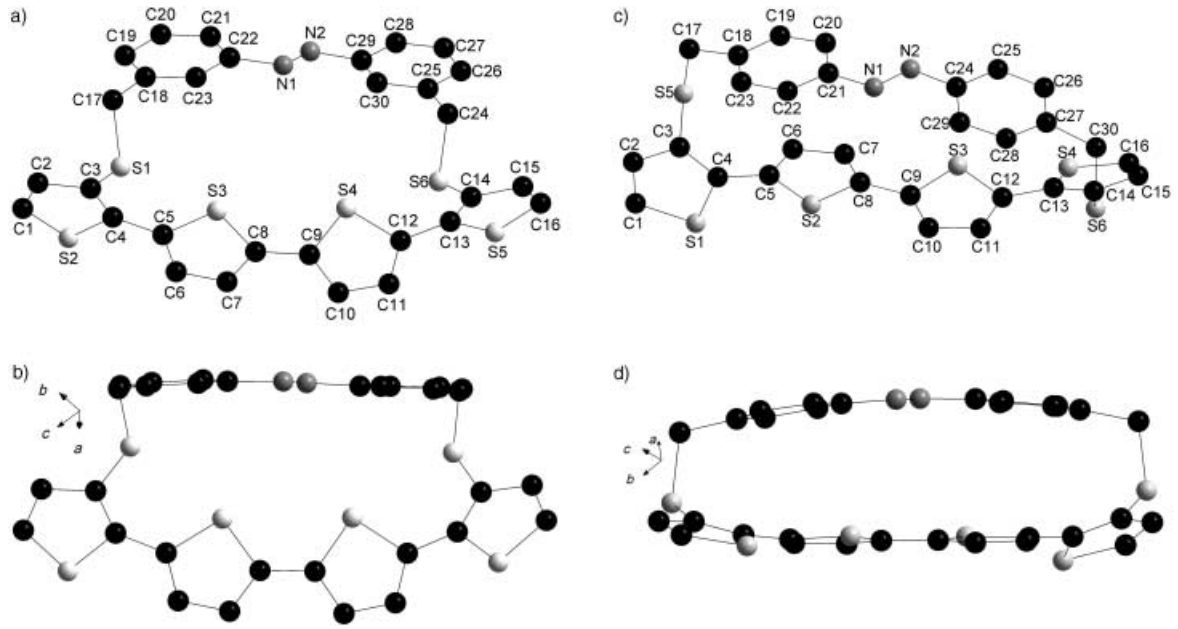

Figure 4. Crystallographic structures of *m*-**4T** (left) and *p*-**4T** (right).

Optical properties: Figure 5 compares the electronic absorption spectra of *p*-**4T** and *m*-**4T** to those of their constituent building blocks namely bis-3,3‴′-cyanoethylsulfanylquaterthiophene **4**, *m*-**2**, and *p*-**2**. The spectrum of **4** has a broad structureless absorption band typical for *n*Ts, with a maximum at 403 nm (Table 1). Dimethylazobenzenes *m*-**2** and *p*-**2** have similar spectra with an intense band corresponding to the π–π* transition with maxima at 324 and 335 nm, respectively, and a weak band with a maximum around 440 nm corresponding to the n–π* transition.[21]

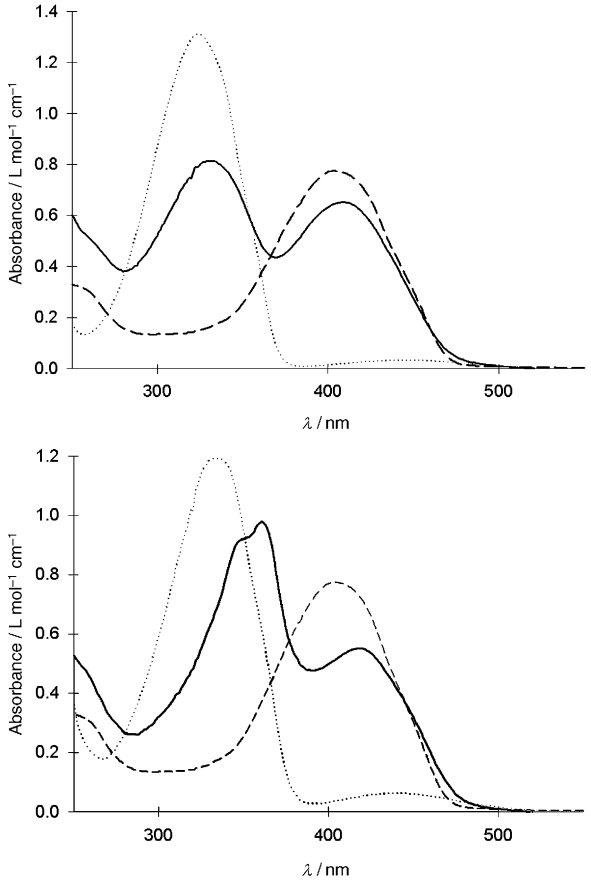

Figure 5. Electronic absorption spectra recorded in CH_2Cl_2. Top: *m*-**4T** (——), *m*-**2** (· · ·), **4** (- - - -). Bottom: *p*-**2** (· · ·), *p*-**4T** (——), **4** (- - - -).

Table 1. UV/Vis spectroscopic data measured in CH_2Cl_2 and fluorescence emission data. Quantum yields were determined at an optical density of 0.05 with perylene in 95% ethanol as standard.

Compound	λ_{max} Azo [nm]	λ_{max} *n*T [nm]	ϕ_{em} [%]
m-**2**	324	–	
p-**2**	335	–	
DPS4T	–	405	16.0
4	–	403	14.4
m-**4T**	327	409	2.00
p-**4T**	360	420	0.90
7	–	452	30.2
p-**6T**	359	457	2.30

Comparison of the UV/Vis spectrum of *m*-**4T** to those of its constitutive parts shows that the λ_{max} of both the azo and 4T systems undergoes a small bathochromic shift of 3 and 6 nm, respectively. Although these shifts may be indicative of weak interactions between the two conjugated systems in the ground state, other factors should also be taken into account such as differences in conformation (***AAA*** for compound **4** and ***ASA*** for *m*-**4T**) and deviation from planarity (see Figures 3 and 4).

Comparison of the UV/Vis data for compounds **4**, *p*-**2**, and *p*-**4T** shows that the red shifts of the λ_{max} of both the azo and the 4T bands (25 and 17 nm, respectively) are significantly larger than for *m*-**4T**. This different behavior strongly suggests that the short distance between the planes containing the azo and 4T system in *p*-**4T** favors through-space π-orbital

interactions in a process similar to that well known for aromatic cyclophanes.[28]

Further evidence for the influence of the mode of fixation of the azo group on its through-space interactions with the 4T chain are given by the photoluminescence properties of the various compounds. The fluorescence-emission quantum yields (ϕ_{em}) of *m*-**4T**, *p*-**4T**, and *p*-**6T** have been measured in CH_2Cl_2 and compared to those of quater- and sexithiophenes **4** and **7**. The ϕ_{em} value of 3,3‴′-dipentylsulfanylquaterthiophene (DPS**4T**) was also measured in order to ascertain the effect of the cyanoethyl groups on the fluorescence properties of the *n*T chain. The measured value of ϕ_{em} for DPS**4T** (16%) agrees well with that reported for dimethylsulfanylquaterthiophene (17%).[29]

The data in Table 1 show that the ϕ_{em} values for the oligomers without azo groups are comparable to those of unsubstituted *n*Ts,[30] and confirm that the cyanoethyl substituents have little influence on the photoluminescence. Conversely, the data for the azo-derivatized compounds clearly show that the azo group induces a dramatic quenching of the fluorescence of the *n*T chain. A closer examination of the data in Table 1 shows that the quenching ratio increases from a factor of 7 for *m*-**4T** to 16 and 13 for *p*-**4T** and *p*-**6T**, respectively. These results suggests that, as expected, the parallel orientation and short distance of the two conjugated systems in *p*-**4T** and *p*-**6T** allow the development of stronger π-orbital through-space interactions.

Photodynamic behavior: The dynamic behavior of *m*-**4T**, *p*-**4T** and *p*-**6T** under photoirradiation has been investigated by UV/Vis and ^{1}H NMR spectroscopy and by cyclic voltammetry. A control experiment performed on a 10^{-4} M solution of *p*-**2** in CH_2Cl_2 shows that, as expected, irradiation with 340 nm monochromatic light causes bleaching of the 335 nm band with an hypsochromic shift of λ_{max} to 305 nm and a slight intensification of the n – π* transition at 439 nm. Return to the initial conditions can be achieved either thermally or by irradiation at 480 nm.

Despite the use of different substrate concentrations, irradiation of *m*-**4T** under the same conditions failed to produce any spectral change. This absence of effect can be explained by the fact that the initial structure of *m*-**4T** is already in a ***ASA*** conformation and therefore, there is no possibility of shortening the S···S distance in order to accommodate the *cis* configuration of the azobenzene group. This locking of the system thus inhibits the isomerization of the azo group.

As shown in Figure 6, irradiation of *p*-**4T** at 360 nm produces a decrease of the intensity of the 360 nm π – π* azo band with an enhancement of the resolution of the vibronic fine structure. Concurrently, the intensity of the 420 nm band corresponding to the superimposition of the n – π* transition of azobenzene and π – π* transition of 4T increases significantly. It is noteworthy that the intensification of this band is considerably larger than that observed with the model azo compound *p*-**2** (not shown). This important difference shows that the intensification of the 420 nm band cannot be attributed to the sole intensification of the n – π* transition of azobenzene.

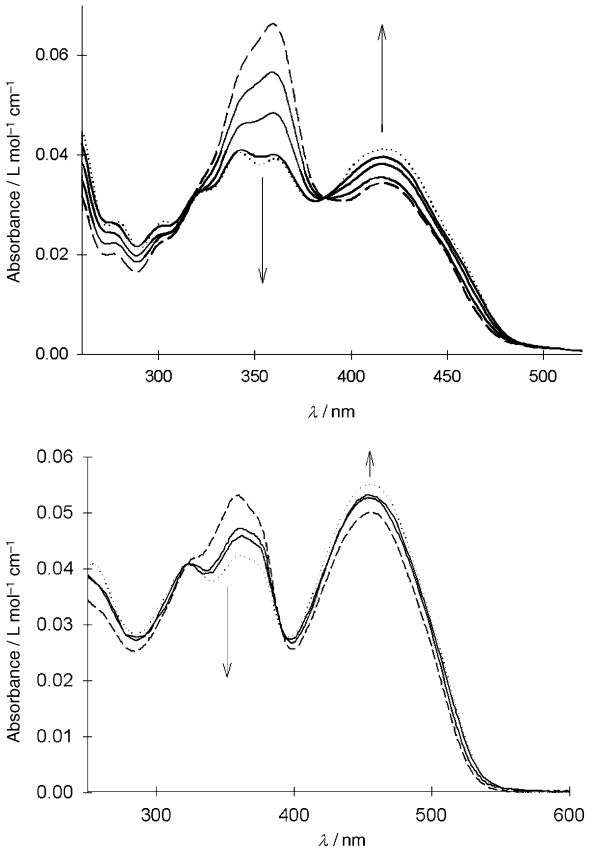

Figure 6. Changes in the UV/Vis spectrum of top: *p*-**4T** (2×10^{-5} M in CH_2Cl_2) and bottom: *p*-**6T** (1.5×10^{-5} M in CH_2Cl_2) during photoirradiation at 360 nm: initial spectrum (- - - -) and after 3 h irradiation at 360 nm (····).

As predicted by modeling, the ***SAS***-to-***ASA*** conformational transition of the 4T chain results in a decrease in the HOMO – LUMO gap and, thus, in a red shift of λ_{max} with an increase in the molecular absorption coefficient. This process was analyzed in detail in a recent theoretical and experimental study of crown-annealed *n*Ts.[18] On the other hand, the spectra in Figure 5 show that, before photoisomerization of the azo group, through-space interactions between the azobenzene and 4T conjugated systems produce a 17 nm red shift of the λ_{max} of the 4T chain. On these grounds, the invariance of the λ_{max} of the 4T chain can be interpreted as the consequence of two counteracting effects, that is, a red shift associated with the ***SAS***-to-***ASA*** conformational transition and a blue shift resulting from the decrease in the through-space interactions with the azobenzene group.

As shown in Figure 6 (bottom), the behavior of *p*-**6T** is qualitatively very similar to that of *p*-**4T**. The smaller magnitude of the change in the intensity of the absorption bands can be attributed to the fact that a part of the π-conjugated chain (i.e., the two terminal thiophene rings) is not involved in the conformational change. Furthermore, because of the limited power of our monochromatic light source, the higher absorption coefficient of *p*-**6T** probably also contributes to limiting the magnitude of the photoisomerization process. For both *p*-**4T** and *p*-**6T**, these spectral changes are fully reversible, and the initial spectrum is recovered after irradiation with 480 nm light.

Figure 7 shows the aromatic region of the ^{1}H NMR spectrum of compound *p*-**4T** in $CDCl_3$ before and after irradiation with a 360 nm monochromatic light. Assignments of the proton chemical shifts of the initial spectrum (Figure 7,

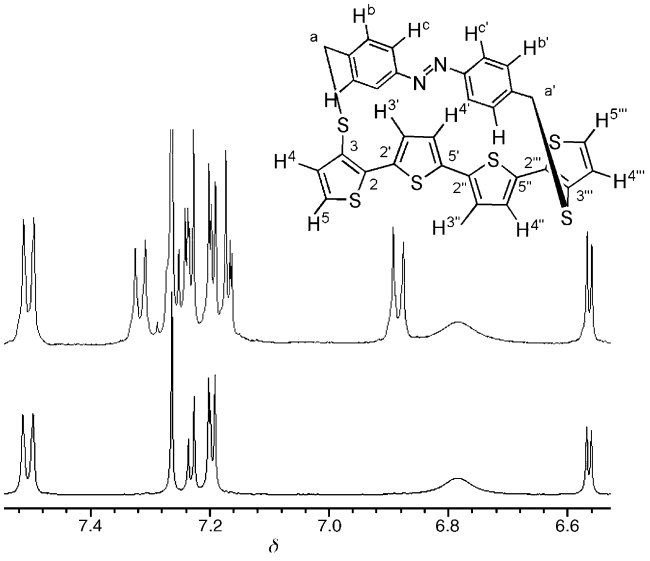

Figure 7. Aromatic region of the ^{1}H NMR spectrum of *p*-**4T** (9×10^{-4} M) in $CDCl_3$. Bottom: initial spectrum, top: after 5 h irradiation with 360 nm monochromatic light.

top) were completed by comparing HMQC, HMBC, and NOESY data; this allowed the following to be firmly identified: Hb/Hb′ ($\delta = 6.73$ ppm, br s or d, $J = 8.5$ Hz, 2H at 333 K,), Hc/Hc′ ($\delta = 7.50$ ppm, d, $J = 8.5$ Hz, 2H), H4/H5‴ ($\delta = 7.23$ ppm, d, $J = 5.0$ Hz, 2H), H5/H4‴ ($\delta = 7.19$ ppm, d, $J = 5.0$ Hz, 2H), H3′/H4″ ($\delta = 7.18$ ppm, d, $J = 4.0$ Hz, 2H), and H4′/H3″ ($\delta = 6.56$ ppm, d, $J = 4.0$ Hz 2H). In this respect, H3′/H4″ were differentiated from H4′/H3″ through the observation of the ^3J correlation to C2/C2‴ that the former shared with H4/H4‴. The unusual upfield chemical shifts of Hb/Hb′ and H4′/H3″ was attributed to their location in the shielding cones of their respective facing thiophenic or benzenic system. After irradiation with 360 nm monochromatic light, the ^{1}H NMR spectrum exhibits additional signals associated with the new geometry of the molecule (Figure 7). The chemical shifts of the Hb/Hb′ couples can be deduced from a 2D dipole–dipole interaction proton correlation analysis (NOESY), which shows a strong nOe between these protons on the one hand and the thiomethylene group on the other.

Thus, the broad singlet for the four Hb/Hb′ protons at $\delta =$ 6.79 ppm becomes a doublet at $\delta = 7.32$ ppm, while the H4′/H3″ doublet is downfield shifted from $\delta = 6.58$ to 7.17 (or 7.23) ppm. These increases in chemical shift are thus related to the corresponding protons exiting the shielding cones of the opposite aromatic systems; this, in turn, is due to the changes in the geometry of the azobenzene and 4T systems. Before irradiation, the NOESY spectrum also shows strong interactions between H3′/H4″ and Hc/Hc′ as well as between H4′/H3″ and Hc/Hc′; this shows the short distances between these various protons.

The disappearance of this nOe after irradiation thus indicates that the isomerization process pushes away protons Hb/Hb′ and H3′/H4″. Integration of the *cis*/*trans* signals shows that after 5 h of irradiation, 47% of compound *p*-**4T** has been isomerized. Irradiation with a 480 nm monochromatic light leads to the disappearance of the new signals formed during the forward process and to the recovery of the initial spectrum. After 3 h of irradiation at 480 nm, only 12% of azobenzene remains in the *cis* configuration. After a complete forward/backward cycle, no new signal appears in the spectrum, thus demonstrating the absence of degradation of the molecule.

Further information on the effects of photoisomerization of the attached azo group on the electronic properties of the *n*T chain have been obtained by analyzing the electrochemical behavior of *p*-**4T** and *p*-**6T** before and after photoirradiation. A control experiment on *p*-dimethylazobenzene *p*-**2** showed that the azo group is electrochemically inert up to +1.70 V versus Ag/AgCl.

The cyclic voltammogram (CV) of *p*-**4T** in methylene chloride in the presence of Bu_4NPF_6 shows a reversible oxidation wave with a redox potential E^0 at 0.94 V, corresponding to the oxidation of 4T into its radical cation (Figure 8). Irradiation at 360 nm produces a progressive

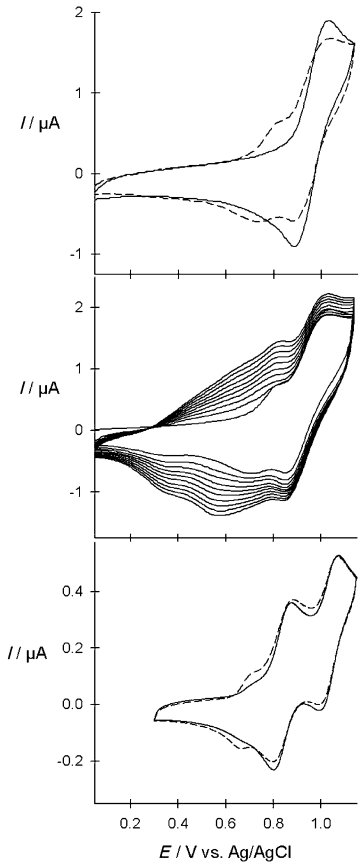

Figure 8. Cyclic voltammograms recorded in 0.1M Bu_4NPF_6/CH_2Cl_2, scan rate 100 mV s^{-1}. Top *p*-**4T** (5×10^{-4} M), before irradiation (····) and after 2 h irradiation at 360 nm (——). Middle: cyclic voltammograms obtained by application of recurrent potential scans to the same solution under irradiation at 360 nm. Bottom: cyclic voltammograms of *p*-**6T** (5×10^{-4} M). Dotted line before irradiation, solid line after 2 h irradiation at 360 nm.

decrease in the intensity of this wave and the emergence of a new redox system at lower potential ($E^0 = 0.78$ V). These changes are fully reversible, and the initial CV can be recovered by irradiation with 480 nm monochromatic light or by a slow thermal process in the dark. These results clearly demonstrate that photoisomerization of the azo group produces conformational changes in the 4T chain that result in an increase of the HOMO level.

Application of recurrent potential scans between 0.00 and +1.10 V to a solution of *p*-**4T** that has been irradiated for 2 hours at 360 nm leads to the growth of a new broad redox system at less positive potential (0.40 to 0.80 V region). This process is accompanied by the electrodeposition of a thin dark film onto the platinum electrode. A control experiment done prior to irradiation confirmed that the initial CV is stable under cycling in the dark and that electrodeposition occurs exclusively after photoisomerization of the attached azo group and hence after the ***SAS***-to-***ASA*** transition of the 4T chain (Scheme 2). This result suggests that the conformational

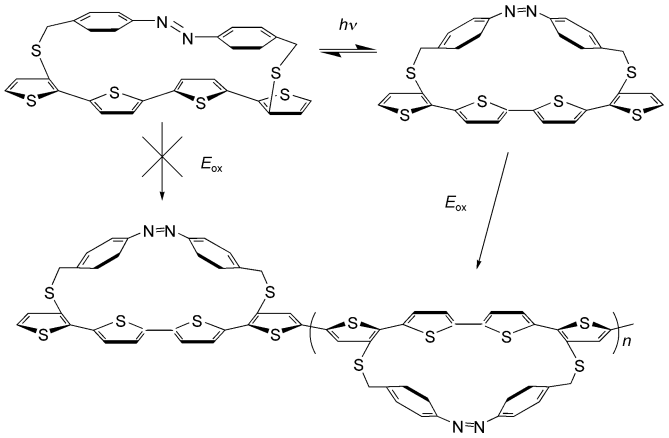

Scheme 2.

switch of the 4T chain enhances the reactivity of the free α-positions of the terminal thiophene rings thus allowing the radical cation to form a more extended π-conjugated system, in a process similar to the electropolymerization of thiophene derivatives.[31]

The CV of *p*-**6T** exhibits two successive one-electron redox processes corresponding to the successive generation of the radical cation and dication at redox potentials $E^0 1$ and $E^0 2$ of 0.85 and 1.04 V. After 2 hours of irradiation at 360 nm, the intensity of the first redox system undergoes a slight decrease, while a new redox system emerges with E^0 at 0.70 V. As for optical experiments, the magnitude of the observed effect is smaller than for *p*-**4T** presumably because of the combined effects of the higher molecular-absorption coefficient of *p*-**6T** and the fact that a part of the π-conjugated system is not involved in the conformational transition. As expected, the application of recurrent potentials under continuous irradiation does not lead to any electrodeposition process. This result confirms that the stabilization of the radical cation associated with chain extension and, of course, the blocking of the terminal α-positions by hexyl chains prevent the chemical coupling of the electrogenerated radical cation.

Conclusion

Quater- and sexithiophenes with a photoisomerizable azobenzene group covalently attached to two fixed positions of the π-conjugated system have been synthesized. Theoretical modeling of the structure and electronic properties provides a powerful tool for the design of molecular architectures that combine synthetic accessibility, conformational flexibility, and, thus, efficient and reversible photomechanical control of the electronic properties of the π-conjugated system through conformational transitions.

In addition to contributing to the enrichment of the toolbox of dynamic molecular devices such as actuators or machines, extension of the concepts developed in this work to other classes of oligomers and polymers can open interesting perspectives for various fields of research including molecular electronics and stimuli-responsive nanostructured materials. Work in this direction is now underway and will be reported in future publications.

Experimental Section

NMR spectra were recorded with a Bruker Avance DRX 500 (^{1}H, 500.13 MHz and ^{13}C, 125.75 MHz). Chemical shifts are given in ppm relative to TMS. IR spectra were recorded with a Perkin–Elmer 841 spectrophotometer and UV/Vis spectra with a Perkin–Elmer Lambda 2 spectrometer. Melting points are uncorrected. Mass-spectrometry analyses were performed on a JMS-700 (JEOL LTD, Akishima, Tokyo, Japan) double-focusing mass spectrometer with reversed geometry and equipped with a pneumatically assisted electrospray ionization (ESI) source. Nitrogen was used as the nebulizer gas. The sample, diluted in a chloroform or in $CHCl_3/CH_3CN$ (70:30), was introduced into the ESI interface with a syringe pump (PHD 2000 infusion; Harvard Apparatus, Holliston, MA, USA) at a 40 μL nm^{-1} flow rate. A 5 kV acceleration voltage was applied, and the elemental composition of the ions was checked by high-resolution measurements by using an electric-field scan with a mixture of PEGs as internal standard and nominal molecular weights centered around 1000.

X-ray data collection was performed at 294 K on an Enraf–Nonius MACH3 four-circles diffractometer equipped with a graphite monochromator utilizing $Mo_{K\alpha}$ radiation ($\lambda = 0.71073$ Å). The structures were solved by direct methods (SIR) and refined on *F* by full-matrix least-squares techniques with MolEN package programs. For the two compounds, absorption was corrected by DIFABS and the H atoms were included in the calculation without refinement. The crystallographic data are given in Table 2.

CCDC-207283 (*m*-**4T**)contains the supplementary crystallographic data for this paper. These data can be obtained free of charge via www.ccdc.cam.ac.uk/conts/retrieving.html (or from the Cambridge Crystallographic Data Centre, 12 Union Road, Cambridge CB2 1EZ, UK; fax: (+44) 1223-336033; or deposit@ccdc.cam.uk).

Irradiation was performed with a 150 W high-pressure Xenon lamp by using band pass filters. The incident light power was X 0.64 mW cm^{-2} at 360 nm and X 1.52 mW cm^{-2} at 480 nm.

Cyclic voltammetry was performed in acetonitrile or dichloromethane purchased from SDS (HPLC grade). Tetrabutylammonium hexafluorophosphate was purchased from Fluka (puriss) and used without purification. Solutions were deaerated by nitrogen bubbling prior to each experiment, which was run under a nitrogen atmosphere. Experiments were performed in a one-compartment cell equipped with a platinum working microelectrode (Ø = 1 mm) and a platinum-wire counter electrode. An Ag/AgCl electrode checked against the ferrocene/ferricinium couple (Fc/Fc^+) before and after each experiment was used as reference. Electrochemical experiments were carried out with a PAR 273 potentiostat with positive feedback compensation.

Materials: 3,3‴-Bis(2-cyanoethylsulfanyl)-2,2′:5′,2″:5″,2‴-quaterthiophene (**4**) was prepared according to the procedure already reported.

Table 2. X-ray experimental data for *m*-**4T**.

Formula	$C_{30}H_{20}N_2S_6$
M_w	600.89
crystal system	orthorhombic
space group	$P2_12_12_1$
a [Å]	8.276(1)
b [Å]	14.258(1)
c [Å]	23.411(4)
α [°]	90
β [°]	90
γ [°]	90
V [Å^3]	2762(1)
Z	4
color	orange
crystal dims [mm]	0.60 × 0.31 × 0.26
D_{calcd} [g cm^{-3}]	1.44
F000	1240
m [mm^{-1}]	0.520
trans. min and max	−0.5274/1.0000
T [K]	294
radiation	$Mo_{K\alpha}$ graphite monochromated
λ [Å]	0.71073
diffractometer	Enraf Nonius CAD4
scan mode	W
hkl limits	−11,0/−20,0/0,32
θ limits [°]	2.5/29.99
number of reflns measured	4536
number of reflns with $I > 3\sigma(I)$	1712
weighting scheme	$4F_o^2/(\Sigma 2(F_o^2) + 0.0064F_o^4)$
number of variables	193
R	0.053
Rw	0.072
GOF	1.329
largest peak in final difference [e Å^{-3}]	0.718

***Trans*-azo-*m*-toluene (*m*-2)**: A pyridine/Cu_2Cl_2 catalyst was prepared by the introduction of anhydrous CuCl (5 g, 0.7 equiv) into anhydrous pyridine (50 mL). The mixture was stirred for 10 min, and the insoluble residue was eliminated by filtration. 3-Toluidine (*m*-**1**; 7 g, 65.3 mmol) was then dissolved in the filtered solution, which was stirred for two hours under O_2 bubbling. After addition of water (200 mL) and Et_2O (150 mL), the organic phase was separated, washed with aqueous HCl (1M), dried (Na_2SO_4), and concentrated. The residue was washed with ethanol to give *m*-**2** (3.0 g, 44%) as an orange solid. M.p. 144–145 °C; ^{1}H NMR ($CDCl_3$) $\delta = 2.44$ (s, 6H), 7.30 (d, $^3J = 8.2$ Hz, 4H), 7.82 (d, $^3J = 8.2$ Hz, 4H); UV/Vis (CH_2Cl_2): λ_{max} ($\log\varepsilon$) = 335 (4.60), 439 nm (3.32).

***Trans*-azo-*p*-toluene (*p*-2)**: This compound was prepared by using the same procedure as above from CuCl (5 g, 0.7 equiv), pyridine (50 mL), and 4-toluidine (*p*-**1**) (7 g, 65.3 mmol). Chromatography on silica gel (CH_2Cl_2) gave *p*-**2** (2.15 g, 32%) as an orange solid. M.p. 55–56 °C; ^{1}H NMR ($CDCl_3$) $\delta = 2.47$ (s, 6H), 7.30 (d, $^3J = 7.4$ Hz, 2H), 7.41 (m, 2H), 7.73 (m, 4H); UV/Vis (CH_2Cl_2): λ_{max} ($\log\varepsilon$) = 324 (4.60), 441 nm (3.32).

***Trans*-1,1′-azobis(4-bromomethylbenzene) (*p*-3)**: A mixture of *p*-**2** (1 g, 4.8 mmol), *N*-bromosuccinimide (NBS) (2.5 g, 2.9 equiv), and benzoyl peroxide (60 mg, 0.01 equiv) in CCl_4 (60 mL) was heated at reflux for 30 min under a N_2 atmosphere. The succinimide formed was separated by filtration of the hot mixture and washed with hot CCl_4. The organic phases were combined, washed with hot water, dried over Na_2SO_4, and evaporated in vacuo. The residue was recrystallized twice from butan-2-one to give 500 mg (28%) of an orange solid. M.p. 217–218 °C; ^{1}H NMR ($CDCl_3$) δ = 4.56 (s, 4H), 7.54 (d, $^3J = 8.3$ Hz, 4H), 7.89 (d, $^3J = 8.3$ Hz, 4H); UV/Vis (CH_2Cl_2): λ_{max} ($\log\varepsilon$) = 334 (4.59), 437 nm (3.30).

***Trans*-1,1′-azobis(3-bromomethylbenzene) (*m*-3)**: This compound was prepared by using the same procedure as above from *m*-**2** (2 g, 9.6 mmol), NBS (5 g, 2.9 equiv), and AIBN (120 mg) in anhydrous CCl_4 (120 mL). Two recrystallizations in CH_3CN, gave 1 g (28%)of an orange solid. M.p. 141–143 °C; ^{1}H NMR ($CDCl_3$) $\delta = 4.59$ (s, 4H), 7.53 (m, 4H), 7.85 (m, 2H), 7.95 (m, 2H); UV/Vis (CH_2Cl_2): λ_{max} ($\log\varepsilon$) = 331 (4.59), 447 nm (3.30).

3,3‴-[*Trans*-1,1′-azobis(4-benzylsulfandiyl)]-2,2′:5′,2″:5″,2‴-quaterthiophene (*p*-4T): A solution of $CsOH \cdot H_2O$ (150 mg, 2.2 equiv) in degassed MeOH (5 mL) was added dropwise to a solution of quaterthiophene **4** (273 mg, 0.54 mmol) in degassed DMF (20 mL) under a N_2 atmosphere. After being stirred for 30 min, this solution and a solution of *p*-**3** (200 mg, 1 equiv) in degassed DMF (25 mL) were added simultaneously, at room temperature and under a N_2 atmosphere, to anhydrous degassed DMF (100 mL) over ca. 6 h by using perfusor pumps. After 10 h of stirring, the reaction mixture was concentrated in vacuo. The residue was dissolved in CH_2Cl_2 (200 mL) and washed with water. After drying (Na_2SO_4), the solution was concentrated in vacuo to give a residue that was separated by chromatography on silica gel (CH_2Cl_2/hexane 1:1). After dissolution of the obtained powder in hot $CHCl_3$/hexane (2:1), addition of cold hexane gave a precipitate that was filtered to give 60 mg (18%) of an orange solid. M.p. >250 °C; ^{1}H NMR ($CDCl_3$) $\delta = 3.79$ (s, 4H), 6.56 (d, $^3J = 3.8$ Hz, 2H), 6.73 (br s, 4H), 7.19 (m, 4H), 7.23 (d, $^3J = 5.1$ Hz, 2H), 7.50 (d, $^3J = 7.6$ Hz, 4H); ^{13}C NMR ($CDCl_3$) δ = 43.2, 123.0, 123.4, 123.8, 123.9, 126.6, 128.9, 133.7, 135.6, 136.3, 140.9, 142.1, 151.3; UV/Vis (CH_2Cl_2): λ_{max} ($\log\varepsilon$) = 360 (4.52), 417 nm (4.30); HRMS (ESI): calcd for $C_{30}H_{20}N_2S_6 + Na^+$: 622.9848; found: 622.9844; elemental analysis calcd (%) for $C_{30}H_{20}N_2S_6$: C 59.96, H 3.35, S 30.02, N 4.66; found: C 59.55, H 3.46, S 30.56, N 4.55.

3,3‴-[*Trans*-1,1′-azobis(3-benzylsulfandiyl)]-2,2′:5′,2″:5″,2‴-quaterthiophene (*m*-4T): This compound was prepared by using the same procedure as above from quaterthiophene **4** (400 mg, 0.8 mmol), CsOH (252 mg, 2.1 equiv), and *m*-**3** (290 mg, 1 equiv). Chromatography on silica gel (CH_2Cl_2/petroleum ether 7:3) gave *m*-**4T** as an orange solid (300 mg, 62.5%). M.p. 229–231 °C; ^{1}H NMR ($CDCl_3$) $\delta = 3.91$ (s, 4H), 6.58 (d, ^3J = 7.1 Hz, 2H), 6.80 (d, $^3J = 3.8$ Hz, 2H), 6.83 (, $^3J = 3.8$ Hzd, 2H), 7.10 (t, ^3J = 7.6 Hz, 2H), 7.18 (d, $^3J = 5.2$ Hz, 2H), 7.20 (d, $^3J = 5.2$ Hz, 2H), 7.63 (d, ^3J = 7.9 Hz, 2H), 7.77 (s, 2H); ^{13}C NMR ($CDCl_3$) δ = 42.2, 122.5, 122.8, 123.3, 123.4, 124.2, 127.6, 127.9, 130.7, 133.1, 134.7, 137.1, 137.9, 142.1, 152.5; UV/Vis (CH_2Cl_2): λ_{max} ($\log\varepsilon$) = 322 (4.52), 409 nm (4.41); MS (70 eV, EI): *m*/*z* (I%): 600 (100) [M^+], 446 (10), 391 (30), 358 (24), 196 (14), 155 (12), 84 (47), 69 (16); HRMS (ESI) calcd for $C_{30}H_{20}N_2S_6$ 599.9951; found 599.9959; elemental analysis calcd (%) for C 59.96, H 3.35, S 30.02, N 4.66; found: C 59.91, H 3.26, S 31.61, N 4.51.

2-Tributylstannyl-5-hexylthiophene (7): A solution of *n*-BuLi (2.5M) in hexane (13 mL, 1.1 equiv) was added dropwise to a solution of 2-*n*-hexylthiophene (**6**; 5 g, 29.7 mmol) in anhydrous THF (20 mL) under N_2 at −25 °C. After 30 min of stirring at −25 °C, Bu_3SnCl (8.5 mL, 1.05 equiv) was slowly added. The reaction mixture was warmed up to room temperature and stirred for 1 h. After dilution with CH_2Cl_2 (60 mL), the organic phase was successively washed with a saturated aqueous NH_4Cl and water, dried over Na_2SO_4, and evaporated in vacuo. The colorless oil (13.3 g, 98%) was directly used in the next step without further purification. ^{1}H NMR ($CDCl_3$) $\delta = 0.92$ (m, 12H), 1.08 (m, 6H), 1.34 (m, 12H), 1.28 (m, 6H), 1.72 (q, $^3J = 7.3$ Hz, 2H), 2.85 (t, $^3J = 7.7$ Hz, 2H), 6.90 (d, $^3J = 3.2$ Hz, 1H), 7.98 (d, $^3J = 3.2$ Hz, 1H).

5,5‴-Dibromo-3,3‴-bis(2-cyanoethylsulfanyl)-2,2′:5′,2″:5″,2‴-quaterthiophene (5): A solution of NBS (0.825 g, 2 equiv) in DMF was added dropwise to a solution of quaterthiophene **4** (1.16 g, 2.32 mmol) in DMF under N_2 at 0 °C in the absence of light. The mixture was stirred 6 h at room temperature and concentrated in vacuo, and the residue was dissolved in CH_2Cl_2 (150 mL). The organic phase was washed with water, dried over Na_2SO_4, and evaporated in vacuo. The orange solid (0.935 g, 61.5%) was directly used in the next step.

5,5⁗-Dihexyl-4′,3‴-bis(2-cyanoethylsulfanyl)-2,2′:5′,2″:5″,2‴:5‴,2⁗:5⁗,2′′′′-sexithiophene (8): A mixture of compounds **5** (0.935 g, 1.43 mmol) and **7** (1.42 g, 2 equiv) plus $Pd(PPh_3)_4$ (500 mg, 0.05 equiv) in anhydrous toluene (50 mL) was heated at reflux 48 h under a N_2 atmosphere. After being cooled, the mixture was concentrated, and the residue was dissolved in CH_2Cl_2, washed with water, dried over Na_2SO_4, and evaporated in vacuo. Chromatography on silica gel (CH_2Cl_2/petroleum ether 8:2) gave **8** as an orange-red solid (310 mg, 26%). M.p. 125–127 °C; ^{1}H NMR ($CDCl_3$) δ = 0.90 (t, $^3J = 6.8$ Hz, 6H), 1.42–1.30 (m, 12H), 1.69 (q, $^3J = 7.5$ Hz, 4H), 2.62 (t, $^3J = 7.3$ Hz, 4H), 2.81 (t, $^3J = 7.6$ Hz, 4H), 3.07 (t, $^3J = 7.3$ Hz, 4H), 6.71 (d, $^3J = 3.5$ Hz, 2H), 7.01 (d, $^3J = 3.5$ Hz, 2H), 7.04 (s, 2H), 7.18 (d, ^3J = 3.9 Hz, 2H), 7.31 (d, $^3J = 3.9$ Hz, 2H); ^{13}C NMR ($CDCl_3$) δ = 14.0, 18.5, 22.6, 28.7, 31.2, 31.5, 31.6, 31.8, 117.8, 123.9, 124.3, 124.5, 125.1, 127.5, 128.4, 133.1, 133.9, 136.1, 137.3, 137.9, 146.8; IR (KBr) 2252 cm^{-1} (CN); UV/Vis (CH_2Cl_2): λ_{max} ($\log\varepsilon$) = 452 nm (4.64); MS MALDI: 832 [M^+].

5,5‴″-Dihexyl-4′,3‴″-[*trans*-1,1′-azobis(4-benzylsulfandiyl)]-2,2′:5′,2″:5″,2‴:5‴,2⁗:5⁗,2⁗′:5⁗′-sexithiophene (*p*-6T): This compound was prepared according the procedure already described for *m*-**4T** from **8** (310 mg, 0.37 mmol), CsOH (130 mg, 2.2 equiv) and *p*-**3** (137 mg, 1 equiv). Chromatography on silica gel (CH_2Cl_2/hexane 1:1) and recrystallization from $CHCl_3$ gave ***p*-6T** as an orange solid (60 mg, 17 %). M.p. $>250\,^{\circ}C$; ^1H NMR ($CDCl_3$) $\delta = 0.92$ (t, $^3J = 6.5$ Hz, 6H), 1.50–1.20 (m, 12H), 1.71 (q, $^3J = 7.4$ Hz, 4H), 2.83 (t, $^3J = 7.5$ Hz, 4H), 3.82 (s, 4H), 6.55 (d, $^3J = 3.8$ Hz, 2H), 6.73 (d, $^3J = 3.4$ Hz, 2H), 5.86 (br s, 4H), 7.03 (d, $^3J = 3.4$ Hz, 2H), 7.19 (m, 4H), 7.50 (d, $^3J = 8.3$ Hz, 4H); UV/Vis (CH_2Cl_2): λ_{max} ($\log\varepsilon$) = 359 (4.61), 457 nm (4.62); MS MALDI: 932 [M^+]; HRMS (ESI) calcd for $C_{30}H_{20}N_2S_6$: 932.1583; found: 932.1611.

Acknowledgement

We would like to thank Rémi de Bettignies for technical assistance, the CINES computing center of Montpellier (France) for the computing time for theoretical calculations. The Ministère de la Recherche et de la Technologie is acknowledged for the Ph.D. grant for B.J. and for financial support of this work (Program Nano-objets individuels).

[1] a) L. A. Bumm, J. J. Arnold, M. Y. Cygan, T. D. Dunbar, T. P. Burgin, L. Jones II, D. L. Allara, J. M. Tour, P. S. Weiss, *Science* **1996**, *271*, 1705–1707; b) M. A. Reed, C. Zhou, C. J. Muller, T. P. Burgin, J. M. Tour, *Science* **1997**, *278*, 252–254; c) C. Kergueris, J.-P. Bourgoin, S. Palacin, D. Esteve, C. Urbina, M. Magoga, C. Joachim, *Phys. Rev. B* **1999**, *59*, 12505–12513.

[2] a) R. M. Metzger, *J. Mater. Chem.* **2000**, *10*, 2027–2036.

[3] *Molecular Switches* (Ed.: B. L. Feringa), Wiley-VCH, Weinheim, **2001**.

[4] C. P. Collier, E. W. Wong, M. Belohradsky, F. M. Raymo, J. F. Stoddart, P. J. Kuekes, R. S. Williams, J. R. Heath, *Science* **1999**, *285*, 391–394.

[5] a) K. E. Drexler, *Nanosystems: Molecular Machinery, Manufacturing and Computation*; Wiley, New-York **1992**; b) Special issue. Movement: molecular to robotic, *Science* **2000**, *288*, 79–106; c) V. Balzani, A. Credi, A. F. M. Raymo, J. F. Stoddart, *Angew. Chem.* **2000**, *112*, 3884–3530; *Angew. Chem. Int. Ed.* **2000**, *39*, 3348–3391; d) J.-P. Sauvage, *Acc. Chem. Res.* **1998**, *31*, 611–619.

[6] J. Clayden, J. H. Pink, *Angew. Chem.* **1998**, *110*, 2040–2043; *Angew. Chem. Int. Ed.* **1998**, *37*, 1937.

[7] a) R. A. Bissel, E. Cordova, A. E. Kaifer, J. F. Stoddart, *Nature* **1994**, *369*, 133–137; b) A. Livoreil, C. O. Dietrich-Buchecker, J.-P. Sauvage, *J. Am. Chem. Soc.* **1994**, *116*, 9399–9400.

[8] T. R. Kelly, H. De Silva, R. A. Silva, *Nature* **1999**, *401*, 150–152.

[9] N. Koumura, R. W. Zijlstra, R. A. van Delden, N. Harada, B. L. Feringa, *Nature* **1999**, *401*, 152–154.

[10] M. C. Jimenez, C. Dietrich-Buchecker, J.-P. Sauvage, A. DeCian, *Angew. Chem.* **2000**, *112*, 3422–3525; *Angew. Chem. Int. Ed.* **2000**, *39*, 3284–3287.

[11] T. Hugel, N. B. Holland, A. Cattani, L. Moroder, S. Markus, H. E. Gaub, *Science* **2002**, *296*, 1103–1106.

[12] a) C. D. Dimitrakopoulos, P. R. L. Malenfant, *Adv. Mater.* **2002**, *14*, 99–117; b) J. A. Rogers, Z. Bao, A. Dodabalapur, B. Crone, V. R. Raju, H. E. Katz, V. Kuck, K. J. Ammundson, P. Drzaic, *Proc. Natl. Acad. Sci.* **2001**, *98*, 4835–4840; c) F. Garnier, *Acc. Chem. Res.* **1999**, *32*, 209–215; d) G. Horowitz, *Adv. Mater.* **1998**, *10*, 365–377; e) H. E. Katz, *J. Mater. Chem.* **1997**, *7*, 369–376; f) F. Garnier, A. Yassar, R. Hajlaoui, G. Horowitz, F. Deloffre, B. Servet, S. Ries, P. Alnot, *J. Am. Chem. Soc.* **1993**, *115*, 8716–8721; g) G. Barbarella, M. Zambianchi, L. Antolini, P. Ostoja, P. Maccagnani, A. Bongini, E. A. Marseglia, E. Tedesco, G. Gigli, R. Cingolani, *J. Am. Chem. Soc.* **1999**, *121*, 8920–8926; h) C. Videlot, J. Ackermann, P. Blanchard, J.-M. Raimundo,P. Frère, M. Allain, R. de Bettignies, E. Levillain, J. Roncali, *Adv. Mater.* **2003**, *15*, 306–310.

[13] a) U. Mitschke, P. Bäuerle, *J. Mater. Chem.* **2000**, *10*, 1471–1507; b) F. Geiger, M. Stoldt, R. Schweiser, P. Bäuerle, E. Umbach, *Adv. Mater.* **1993**, *5*, 922–925; b) G. Barbarella, L. Favaretto, G. Sotgiu, P. Zambianchi, A. Bongini, C. Arbizzani, M. Mastragostino, M. Anni, G. Gigli, R. Cingolani, *J. Am. Chem. Soc.* **2000**, *122*, 11971–11978; c) G. Barbarella, L. Favaretto, G. Sotgiu, L. Antolini, G. Gigli, R. Cingolani, A. Bongini, *Chem. Mater.* **2001**, *13*, 4112–4122.

[14] a) A. Aviram, *J. Am. Chem. Soc.* **1988**, *110*, 5687–5692; b) J. Guay, A. Diaz, R. Wu, J. M. Tour, *J. Am. Chem. Soc.* **1993**, *115*, 1869–1874; c) J. M. Tour, *Chem. Rev.* **1996**, *96*, 537–553; d) J. Roncali, *Acc. Chem. Res.* **2000**, *33*, 147–156; e) I. Jestin, P. Frère, P. Blanchard, J. Roncali, *Angew. Chem. Int. Ed.* **1998**, *37*, 942–945; *Angew. Chem.* **1998**, *110*, 990–993; g) I. Jestin, P. Frère, N. Mercier, E. Levillain, D. Stiévenard, J. Roncali, *J. Am. Chem. Soc.* **1998**, *120*, 8150–8158.

[15] R. H. Baughman, *Synth. Met.* **1996**, *78*, 339–353.

[16] J. M. Marsella, R. J. Reid, S. Estassi, L.-S. Wang, *J. Am. Chem. Soc.* **2002**, *124*, 12507–12510; b) M. J. Marsella, *Acc. Chem. Res.* **2002**, *35*, 944–951.

[17] B. Jousselme, P. Blanchard, E. Levillain, J. Delaunay, M. Allain, P. Richomme, D. Rondeau, N. Gallego-Planas, J. Roncali, *J. Am. Chem. Soc.* **2003**, *125*, 1363–1370.

[18] a) J.-L. Brédas, G. B. Street, B. Thémans, J. M. André, *J. Chem. Phys.* **1985**, *83*, 1323–1329; b) P. M. Viruela, R. Viruela, E. Orti, J.-L. Brédas, *J. Am. Chem. Soc.* **1997**, *119*, 1360–1369.

[19] B. Jousselme, P. Blanchard, E. Levillain, J. Delaunay, M. Allain, P. Richomme, N. Gallego-Planas, J. Roncali, *J. Am. Chem. Soc.* **2003**, *125*, 2888–2889.

[20] G. S. Hartley, *Nature* **1937**, *140*, 281–283.

[21] H. Rau, *Angew. Chem.* **1973**, *85*, 248–258; *Angew. Chem. Int. Ed. Engl.* **1973**, *12*, 224–235; G. S. Kumar, D. C. Neckers, *Chem. Rev.* **1989**, *89*, 1915–1925; b) Y. Nabeshima, A. Shishido, A. Kanazawa, T. Shiono, T. Ikeda, T. Hiyama, *Chem. Mater.* **1997**, *9*, 1480–1487; c) M. Zagorska, I. Kulszewicz-Bajer, A. Pron, J. Sukiennik, P. Raimond, F. Kajzar, A.-J. Attias, M. Lapkoski, *Macromolecules* **1998**, *31*, 9146–9153; d) A. Izumi, R. Nomura, T. Masuda, *Macromolecules* **2001**, *34*, 4342–4347.

[22] a) D. M. Junge, D. V. McGrath, *Chem. Commun.* **1997**, 857–858; b) D.-L. Jiang, T. Aida, *Nature* **1997**, *388*, 454–455; c) A. Archut, G. C. Azzellini, V. Balzani, L. De Cola, F. Vögtle, *J. Am. Chem. Soc.* **1998**, *120*, 12187–12191; d) D. Grebel-Kohler, D. Liu, S. De Feyer, V. Enkelmann, T. Weil, C. Engels, C. Samin, K. Müllen , F. C. De Schryver, *Macromolecules* **2003**, *36*, 578–590.

[23] P. A. van Hal, E. H. A. Beckers, S. C. J. Meskers, R. A. J. Janssen, B. Jousselme, P. Blanchard, J. Roncali, *Chem. Eur. J.* **2002**, *8*, 5415–5429.

[24] P. Blanchard, B. Jousselme, P. Frère, J. Roncali, *J. Org. Chem.* **2002**, 67, 3961–3964.

[25] A. P. Terent'ev, Y. D. Mogilyanskii, *Dokl. Akad. Nauk S.S.S.R.* **1955**, 10391–10393.

[26] Gaussian 98 (Revision A.9), M. J. Frisch, G. W. Trucks, H. B. Schlegel, G. E. Scuseria, M. A. Robb, J. R. Cheeseman, V. G. Zakrzewski, J. A. Montgomery, R. E. Stratmann, J. C. Burant, S. Dapprich, J. M. Millam, A. D. Daniels, K. N. Kudin, M. C. Strain, O. Farkas, J. Tomasi, V. Barone, M. Cossi, R. Cammi, B. Mennucci, C. Pomelli, C. Adamo, S. Clifford, J. Ochterski, G. A. Petersson, P. Y. Ayala, Q. Cui, K. Morokuma, D. K. Malick, A. D. Rabuck, K. Raghavachari, J. B. Foresman, J. Cioslowski, J. V. Ortiz, A. G. Baboul, B. B. Stefanov, G. Liu, A. Liashenko, P. Piskorz, I. Komaromi, R. Gomperts, R. L. Martin, D. J. Fox, T. Keith, M. A. Al-Laham, C. Y. Peng, A. Nanayakkara, C. Gonzalez, M. Challacombe, P. M. W. Gill, B. G. Johnson, W. Chen, M. W. Wong, J. L. Andres, M. Head-Gordon, E. S. Replogle, J. A. Pople, Gaussian; Inc., Pittsburgh, PA, **1998**.

[27] F. van Bolhuis, H. Wynberg, E. E. Havinga, E. W. Meijer, E. G. J. Staring, *Synth. Met.* **1989**, *30*, 381–389; b) P. A. Chaloner, S. R. Gunatunga, P. B. Hitchcock, *Acta Crystallogr. Sect. C* **1994**, *50*, 1941; c) M. Pelletier, F. Brisse, *Acta Crystallogr. Sect. C* **1994**, *50*, 1942–1945.

[28] a) D. J. Cram, N. L. Allinger, H. J. Steinberg, *J. Chem. Soc.* **1953**, *76*, 6132–6141; b) D. J. Cram, H. Steinberg, *J. Am. Chem. Soc.* **1951**, *73*, 5691–5704; c) G. P. Bartholomew, G. C. Bazan, *Acc. Chem. Res.* **2001**, *34*, 30–39, and references therein.

[29] P. Bäuerle, G. Götz, A. Synowczyk, J. Heinze, *Liebigs Ann.* **1996**, 279–284.

[30] R. S. Becker, J. Seixas de Melo, A. L. Maçanita, F. Elisei, *Pure Appl. Chem.* **1995**, *67*, 9–16.

[31] J. Roncali, *Chem. Rev.* **1992**, *92*, 711–738.

Received: April 1, 2003 [F5010]

